UNIVERSITY OF AMSTERDAM

Report

Computational Finance

Lab Assignment #1

Sunday 13th July, 2025 14:00

Student(s):

Maarten Stork (15761770)
Lucas Keijzer (14041073)
Pemmasani Prabakaran Rohith Saai (14968061)

Details:

Lecturers: Sven Karbach & Drona Kandhai

Course: Computational Finance

Course Code: 5284COFI6Y

Introduction

This report is structured into three sections, each corresponding to one of the assigned tasks for the Computational Finance course at the University of Amsterdam. Every section addresses a different question and includes a brief introduction to provide context and guide the reader through the analysis. For full implementation details, see the complete code on GitHub.[1]

In Section 1 (split up into methods, results and discussion), we analyze MSFT's market volatility using real data by estimating 30-day rolling classical and Parkinson volatility, comparing these realized measures to option-implied volatility from the skfolio dataset, constructing a model-free VIX series, and exploring regression relationships with SPX returns.

In Section 2 (made up of a step-for-step writing out of a proof) we solve the Black-Scholes PDE, which is a foundational model in quantitative finance for option pricing. We do this under terminal condition $C(s,T) = s^2$. After this we determine the portfolio holdings ξ_t and η_t in the risky asset S_t and the riskless asset A_t (with $A_t = A_0 e^{rt}$).

In Section 3 (split into introduction, methods and results), we introduce the delta-hedging strategy for options and identify the effect hedging frequency on the profit-and-loss using the Euler method, We also analyze the effect of mismatch volatility between the underlying and delta valuation on the profit-and-loss. Finally, we conduct a theoretical analysis to identify the conditions under which mismatched volatility leads to the final profit=and-loss to vanish to zero.

A concluding section at the end of this report will synthesize the findings and present the conclusions for each of the tasks, summarizing the key insights and implications derived from the analyses above.

[1] See source code and documentation at: https://github.com/Lucas-Keijzer/CompFinance_ass_1

1 Financial Data Science

1.1 Methods

1.1.1 Asset Mean and Volatility: Firstly, we analyze the historical performance of Microsoft Corporation (MSFT) using daily price data from 2010 to the present, obtained via the package[2] (which retrieves data from Yahoo Finance). MSFT is selected because it is a long-established, widely traded stock with robust historical and options market data, making it ideal for our volatility analysis.

In our implementation, we assume uniform daily time intervals (i.e., $\Delta t = 1/252$ years, based on 252 trading days per year). This assumption simplifies the calculation of the classical estimators. We compute the historical mean (or drift) using the classical estimator (Hull, 2015):

$$\hat{\mu}_N = \frac{1}{N} \sum_{k=0}^{N-1} \frac{1}{t_{k+1} - t_k} \left(\frac{S_{k+1} - S_k}{S_k} \right), \tag{1}$$

and the classical realized variance as follows:

$$\hat{\sigma}_N^2 = \frac{1}{N-1} \sum_{k=0}^{N-1} \frac{1}{t_{k+1} - t_k} \left(\frac{S_{k+1} - S_k}{S_k} - \Delta t \, \hat{\mu}_N \right)^2, \tag{2}$$

with the annualized volatility given by $\hat{\sigma}_N = \sqrt{\hat{\sigma}_N^2}$.

Additionally, to capture intra-day variability more robustly (and to reduce sensitivity to discrete jumps), we implement the Parkinson method (Parkinson, 1980):

$$\sigma_{\text{Parkinson}} = \sqrt{\frac{1}{4 \ln(2) \, T} \sum_{t=1}^{T} \left[\ln \left(\frac{h_t}{l_t} \right) \right]^2}, \tag{3}$$

where T is the number of days, and h_t and l_t are the daily high and low prices. The use of a 30-day rolling window allows us to assess short-term volatility dynamics and track time-varying behavior. In the research that follows, every 30-day "realized volatility" series refers to the classical estimator from Eq.(2). The Parkinson estimator (Eq.(3)) is used for the comparisons in Sections 1.3.2 and 1.3.3.

1.1.2 Realized and Implied Volatility: We compare MSFT's forward-looking implied volatility (Black & Scholes, 1973)—extracted from option prices via the `skfolio` dataset[3]—with two backward-looking realized measures: (a) the classical 30-day rolling close-to-close volatility (Eq. (2)) and (b) the 30-day Parkinson range-based volatility (Eq. (3)), both annualized by $\sqrt{252}$. All three series are aligned on common trading dates to support Pearson correlation and cointegration analyses, thereby contrasting market expectations with historical price behavior.

1.1.3 VIX Time Series: We further construct a volatility index time series using real market data for the S&P 500 (SPX). Following the methodology outlined in the CBOE VIX whitepaper (Chicago Board Options Exchange, 2003), we retrieve SPX and VIX data via the `yfinance` package while fixing our analysis date to March 5, 2025. We extract one year of daily historical SPX data and use the SPX closing price on the final

[2] See source code and documentation at: `https://github.com/ranaroussi/yfinance`
[3] See source code and documentation at: `https://github.com/EAIBOT/skfolio`

trading day to compute the forward price via

$$F_0 = S_0 e^{rT}, \tag{4}$$

where S_0 is the SPX spot price, $r = 0.02$ is the risk-free rate, and $T = 1$ year.

For estimating the VIX, we encounter a modeling issue: SPX options do not expire exactly every 30 days but on fixed weekdays (typically Thursdays) (PAP handelt ze elke dag, wel elke dag expiren, die heeft gewoon iedere dag, maar niet weekend), so on many days no option chain is available with exactly 30 days to expiry. In such cases, one may either interpolate between available expiries or choose the closest available expiry. In our analysis, for March 5, 2025, we select the closest available option chain with an expiry date of April 14, 2025. Note that this results in an expiry of 41 days, slightly longer than the ideal 23–37 day range per CBOE methodology (Chicago Board Options Exchange, 2003); this deviation is due to data availability constraints and is documented in our report. For the remainder of the time series, we rely on the official VIX values from `yfinance`.

We then apply the model-free VIX formula:

$$\mathrm{VIX}_t = \sqrt{\frac{2e^{r\tau}}{\tau}\left(\int_0^{F_{t,t+\tau}} \frac{P(t,t+\tau,K)}{K^2}\,dK + \int_{F_{t,t+\tau}}^{\infty} \frac{C(t,t+\tau,K)}{K^2}\,dK\right)}, \tag{5}$$

with $\tau = \frac{30}{365}$ (in years). In our baseline implementation, the integrals are discretized using the `lastPrice` field. To improve accuracy, we refine the estimator by (i) using the midpoint between bid and ask prices, (ii) filtering out options with missing or zero/negative mid-prices, and (iii) restricting the strike range to within $\pm 20\%$ of F_0.

1.1.4 Comparing MSFT Realized Volatility to the VIX Time Series: To explore the relationship between individual-stock volatility and market-implied volatility, we compare MSFT's rolling 30-day realized volatility with the CBOE-quoted VIX. Although the VIX is derived from SPX options—thus reflecting overall market expectations—and MSFT's volatility is specific to a single stock, their comparison provides insights into broader market dynamics during periods of stress. Our methodology involves dual-axis plotting of both series, and we then conduct correlation and cointegration analyses on the aligned time series to quantify their long-term relationship.

1.1.5 Regression Analysis: SPX Returns and Volatility Measures: Finally, we investigate how SPX returns respond to three volatility signals: (1) the level of forward-looking implied volatility (the CBOE VIX), (2) the daily change in implied volatility (ΔVIX), which captures volatility surprises, and (3) the historical realized variance (30-day rolling, annualized). For each measure, we align dates and run an OLS regression of SPX daily returns on the volatility regressor. We include ΔVIX because a sudden spike (or drop) in market-implied vol often has a more direct "fear-shock" effect on prices than the persistent level alone. To ensure model validity, we perform Breusch–Pagan (Breusch & Pagan, 1979) tests for heteroscedasticity and Augmented Dickey–Fuller (Dickey & Fuller, 1979) tests for residual stationarity. This framework allows us to compare the explanatory power of backward-looking versus forward-looking—and surprise—volatility measures on equity returns.

Estimator	Result
Classical Mean (Equation (1))	0.19910
Classical Volatility (Equation (2))	0.25740
Parkinson Volatility (Equation (3))	0.20458

Table 1: Full-sample estimates of historical mean and volatility (annualized) for MSFT.

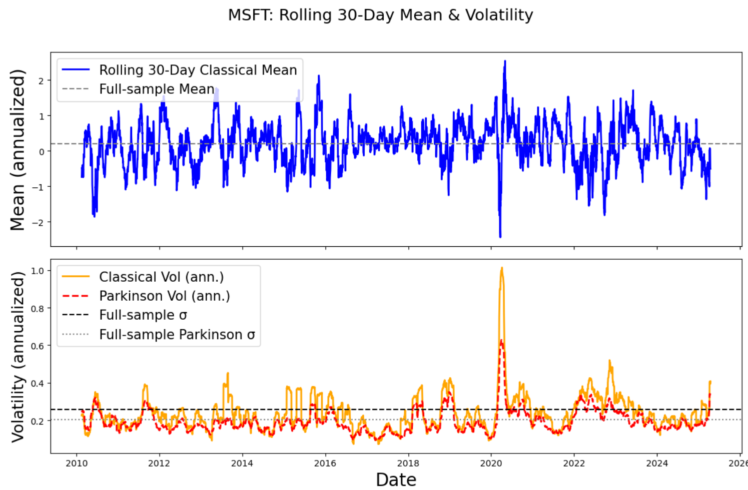

Figure 1: Rolling 30-day estimates for MSFT: classical mean (top), classical volatility and Parkinson volatility (bottom), with the full sample mean and full sample σ shown for reference.

1.2 Results

Table 1 reports the full-sample estimates for MSFT. The classical mean is 0.19910 (roughly 20% annualized drift), and the classical volatility is 0.25740. The Parkinson volatility is lower (at 0.20458), reflecting its range-based smoothing of intraday moves.

Rolling 30-day estimates in Figure 1 show that classical volatility and drift vary significantly over time, especially during market stress, while Parkinson volatility remains (relatively) smoother and lower.

As shown in Figure 2 (and visualized in Figure 3), both realized volatility measures track implied volatility very closely: the classical 30-day close-to-close estimator exhibits a strong positive correlation ($r = 0.706$, $p \approx 0$), while the Parkinson range-based estimator is even more tightly linked ($r = 0.783$, $p \approx 0$).

Figure 4 shows that MSFT's 30-day realized volatility and the CBOE VIX co-move closely, particularly during systemic shocks. The Pearson correlations are approximately $r = 0.65$ (classical) and $r = 0.74$ (Parkinson). An Engle–Granger cointegration test yields an ADF t-statistic of about -3.9 with $p < 0.001$, rejecting the null of no cointegration at the 1% level and confirming a significant long-run equilibrium relationship.

From this point onward, we focus on MSFT's 30-day realized volatility as computed by the classical close-to-close estimator. Applying the model-free VIX formula (Eq.5), yields a baseline estimate of 62.90, which is markedly higher than the CBOE-quoted VIX of 23.51. After improving our inputs—by using mid-quote prices, filtering out invalid or stale options, and restricting strikes to within ±20% of the forward price—the VIX estimate converges to 34.59 (see Table2).

Table 3 shows that while the VIX level (classical calculation) has a small but statistically significant negative effect on SPX returns, and realized variance contributes almost no explanatory power, the ΔVIX

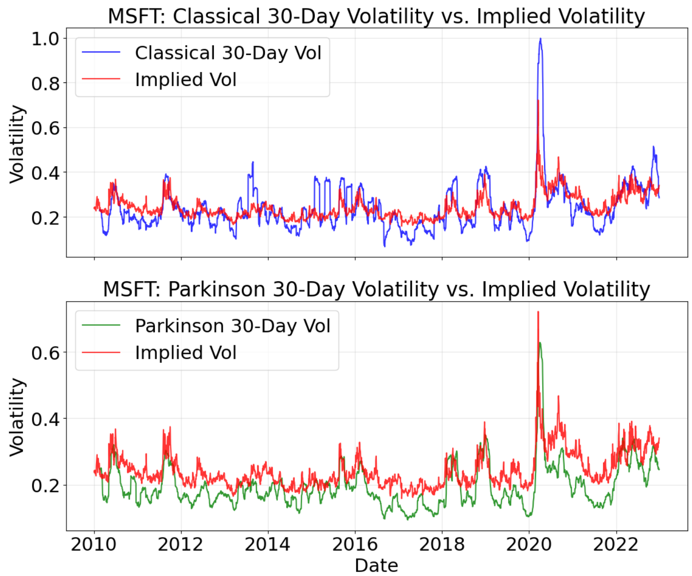

Figure 2: MSFT 30-day rolling realized volatility vs. implied volatility. Top: classical close-to-close estimator. Bottom: Parkinson range-based estimator.

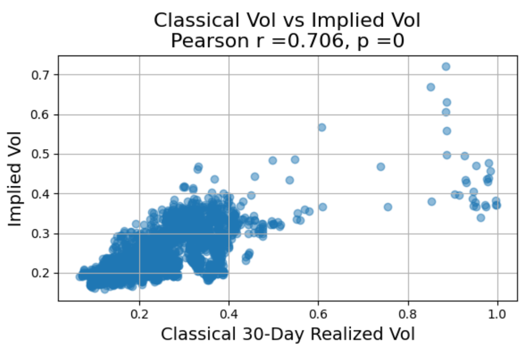

(a) *Classical close-to-close 30-day realized volatility vs. implied volatility.*

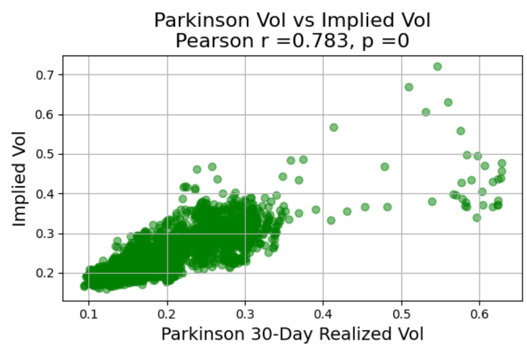

(b) *Parkinson range-based 30-day realized volatility vs. implied volatility.*

Figure 3: Scatter-and-Pearson correlation between MSFT's 30-day realized volatility and its implied volatility.

model captures the bulk of daily return variation. Figure 5 displays the corresponding scatterplots and fitted lines. From the diagnostics in Table 3, the VIX-level and realized-variance regressions exhibit heteroscedastic residuals, whereas the ΔVIX model does not; all three models yield stationary residuals (the Breusch–Pagan test null is homoscedasticity ($p<0.001$ rejects), and the ADF test null is a unit root in the residuals ($p<0.001$ rejects)).

1.3 Discussion

1.3.1 Asset Mean and Volatility: The full-sample results in Table 1 indicate an annualized classical mean of 0.19910 and volatility of 0.25740 for MSFT, reflecting a long-run return of approximately 20% with moderate variability. The annualized Parkinson estimator is 0.20458—lower than the classical measure-based smoothing of intraday extremes. Figure 1 supports this by showing the Parkinson series (dashed red line in the bottom panel) closely tracks classical volatility (solid orange), yet is somewhat lower and exhibits less

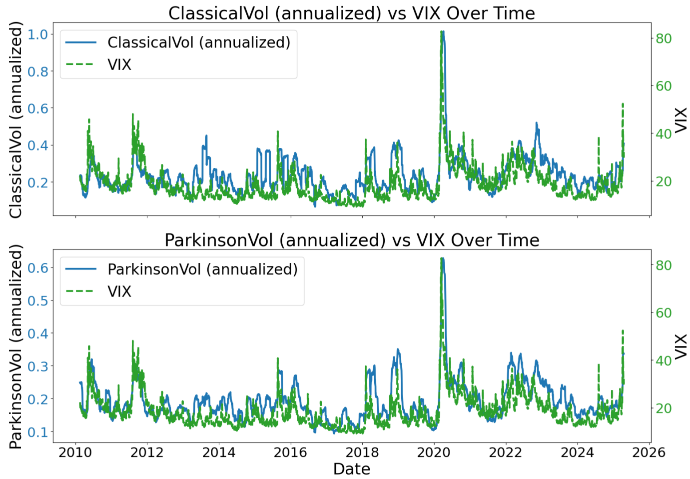

Figure 4: Comparison of MSFT 30-Day Realized Volatility and the CBOE VIX on dual Y-axes.

Quantity	**Baseline**	**Refined**
SPX Spot Price S_0	5778.15	—
Forward Price F_0 (1-Year)	5894.88	—
CBOE Quoted VIX	23.51	—
Estimated VIX (Eq. 5)	62.90	34.59

Table 2: Input data and comparison of baseline vs. refined VIX estimates.

	VIX Level	**Realized Var.**	**ΔVIX**
	Regression Estimates		
Constant	0.0051	0.0003	0.0005
Beta	–0.0003	0.0060	–0.0047
R^2	0.026	0.001	0.638
	Residual Diagnostics		
BP LM Stat.	959.10	578.56	0.03
BP p-value	<0.001	<0.001	0.87
ADF Stat.	–10.72	–12.96	–13.44
ADF p-value	<0.001	<0.001	<0.001

Table 3: OLS regression results and residual diagnostics for SPX daily returns on three volatility measures.

pronounced spikes during market shocks. The classical estimator reacts more sharply to discrete jumps, while Parkinson's lower sensitivity under stress suggests it may be more efficient in normal conditions, whereas classical volatility better captures tail risks—motivating potential hybrid or regime-switching approaches.

1.3.2 Realized and Implied Volatility: Figure 2 plots MSFT's 30-day rolling realized volatilities—classical close-to-close (blue) and Parkinson range-based (green)—against its implied volatility from the `skfolio` dataset. The classical estimator co-moves very closely, while the Parkinson estimator actually exhibits an even stronger link. In both panels, implied volatility typically jumps first (for example, in the early days of the COVID-19 crash), reflecting its forward-looking nature, and the realized measures rise thereafter. The Parkinson series' smoother profile makes it more robust to intraday noise but can delay its response to sudden market shocks.

1.3.3 VIX Time Series: The VIX estimation highlights the sensitivity of model-free implied volatility to input quality. As seen in Table 2, the baseline estimator (using raw `lastPrice` quotes) produced an inflated VIX of 62.90, vastly overstating the CBOE-quoted value of 23.51. After refining the process by filtering stale prices and using bid-ask midpoints, the VIX estimate falls to 34.59—much closer to the true value.

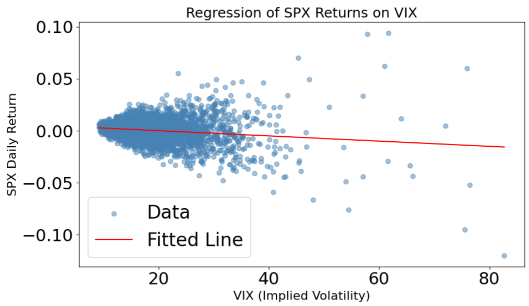

(a) *SPX returns vs. VIX with regression line.*

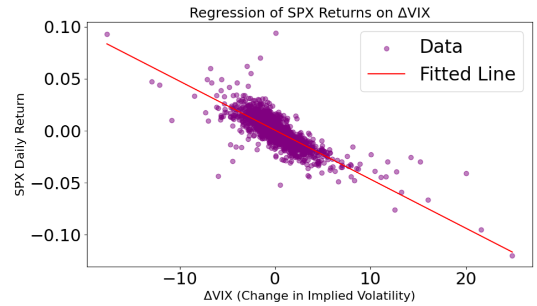

(b) *SPX returns vs.* Δ *VIX with regression line.*

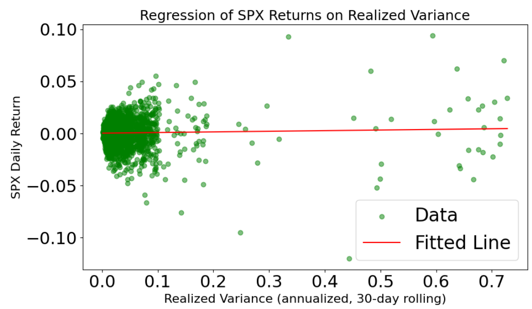

(c) *SPX returns vs. realized variance with regression line.*

Figure 5: SPX daily returns plotted against three volatility measures: (a) VIX level, (b) change in VIX (ΔVIX), and (c) realized variance (30-day rolling).

This 45% reduction demonstrates the importance of filtering noise when working with real options data. Figure 4 also reveals that despite tracking different assets (SPX vs. MSFT), the CBOE VIX and MSFT's realized volatility tend to move in tandem, particularly during macroeconomic shocks (Whaley, 2000). An Engle–Granger cointegration test (p <0.001, lag=1) confirms a statistically significant long-run equilibrium relationship, even though short-term deviations occur.

1.3.4 Comparing MSFT Realized Volatility to the VIX Time Series: Figure 4 shows that both MSFT's 30-day realized volatility and the CBOE VIX spike around the same times, reinforcing that market-wide fear affects both individual stocks and indices. Despite different underlying assets and slightly different horizons, both measures exhibit parallel dynamics and volatility clustering during major events like 2011's Eurozone crisis and the 2022 inflation-driven selloff (Whaley, 2000). This co-movement justifies using the VIX as a market-wide risk proxy even for single-stock applications.

Table 3 confirms three key findings. First, the VIX level has a small but significant negative slope ($\beta = -0.0003$) and explains only 2.6% of daily return variation, showing that a static fear gauge adds little predictive value. Second, backward-looking realized variance performs even worse ($\beta = 0.0060$, $R^2 = 0.1\%$), underscoring that ex post volatility seldom forecasts equity moves. Finally—and most importantly—volatility surprises (ΔVIX) dominate, capturing 63.8% of return variability ($\beta = -0.0047$), with homoscedastic, stationary residuals (BP $p = 0.87$, ADF $p < 0.001$). In practice, this suggests that modelling or hedging SPX returns is far more effective when based on innovations in market fear rather than on its level or on historical measures.

2 Solving the Black–Scholes PDE

In this part we try to solve the following equation:

$$r\,C(s,t) = \frac{\partial C}{\partial t}(s,t) + r\,s\,\frac{\partial C}{\partial s}(s,t) + \frac{1}{2}\sigma^2 s^2\,\frac{\partial^2 C}{\partial s^2}(s,t)$$

for $s > 0$ and $t \in [0, T]$, subject to the terminal condition

$$C(s,T) = s^2$$

and then determine the function $f(t)$.

2.1 Derivatives

Since:	$C(s,t) = s^2\,f(t)$
The 'time-derivative' is:	$C_t(s,t) = s^2 f'(t)$
The 'First spatial' derivative is:	$C_s(s,t) = \frac{\partial}{\partial s}\left[s^2\,f(t)\right] = 2s\,f(t)$
The 'Second spatial' derivative is:	$C_{ss}(s,t) = \frac{\partial^2}{\partial s^2}\left[s^2\,f(t)\right] = 2f(t)$

2.2 Substitute

Now we subsitute these equations into the black-scholes PDE

$$r\,s^2 f(t) = s^2 f'(t) + rs \cdot 2s\,f(t) + \frac{\sigma^2}{2}s^2 \cdot 2f(t)$$

And dividing through by s^2 (since $s > 0$) gives:

$$r\,f(t) = f'(t) + 2r\,f(t) + \sigma^2\,f(t) \quad \text{which is:} \quad f'(t) = -\left(r + \sigma^2\right)f(t)$$

2.3 Solving

$f'(t) = -\left(r + \sigma^2\right)f(t)$ is a standard first-order linear ordinary differential equation, for which the general solution is:

$$f(t) = A\,e^{-(r+\sigma^2)t},$$

where A is a constant. To determine A, we apply the terminal condition $C(s,T) = s^2$:

$$C(s,T) = s^2 f(T) = s^2 \quad \Longrightarrow \quad f(T) = 1.$$

Thus,

$$A\,e^{-(r+\sigma^2)T} = 1 \quad \Longrightarrow \quad A = e^{(r+\sigma^2)T}.$$

Substituting back, we obtain

$$f(t) = e^{(r+\sigma^2)(T-t)},$$

Thus the option price is given by:

$$C(s,t) = s^2\,e^{(r+\sigma^2)(T-t)}$$

2.4 Replicating Portfolio

To replicate the derivative contract, we express the portfolio value as:

$$V_t = \xi_t S_t + \eta_t A_t$$

with the riskless asset given by $A_t = A_0 e^{rt}$, and require that

$$V_t = C(S_t, t) = S_t^2\, e^{(r+\sigma^2)(T-t)}$$

Next, the riskless asset holding η_t is determined by:

$$\eta_t A_t = C(S_t, t) - \xi_t S_t$$

that is,

$$\eta_t e^{rt} = S_t^2\, e^{(r+\sigma^2)(T-t)} - 2S_t^2\, e^{(r+\sigma^2)(T-t)} = -S_t^2\, e^{(r+\sigma^2)(T-t)}$$

Hence,

$$\eta_t = -S_t^2\, e^{(r+\sigma^2)(T-t)-rt}$$

3 Hedging: Volatility Mismatch

3.1 Introduction

Delta-hedging strategy is a trading technique where the option's writer neutralize an option's sensitivity to small moves in the price of its underlying asset. This is done by utilizing the option's delta (Δ), which measures how much the option's price changes for a small change in the underlying:

$$\Delta = \frac{\partial C(t, S_t)}{\partial S_t}$$

This strategy is employed by holding an offsetting amount of the underlying—typically selling shares for each call option (or buying Δ shares for each put) so that the net first-order exposure to S is zero. This dynamic re-hedging removes most of the directional risk, leaving the writer primarily exposed to Γ (curvature) and ν (volatility) risk. In this section, we evaluate the effect of the hedging frequency, volatility mismatch in delta valuation as well as the theoretical analysis of the average profit-and-loss due to this mismatch.

3.2 Methods

To identify the effect of the different hedging frequency and mismatched volatility, we consider a short position in a European call option on a non-dividend paying stock. The option has a maturity of one year and strike K = 99 EUR. Let the one-year risk-free interest rate be 6%, current stock price be 100 EUR and volatility of 20%. We employ the Euler's method for 1000 simulations per experimental setup to simulate different stock price path. Firstly, we evaluate the effect of hedging frequency on the total profit-and-loss of the delta-hedging strategy by hedging daily, weekly, monthly and quarterly while matching the volatility between the underlying and the delta valuation. Secondly, we evaluate the effect of mismatched volatility between the underlying and the delta valuation by varying the delta valuation volatility by 5%, 10%, 20%, 40% and

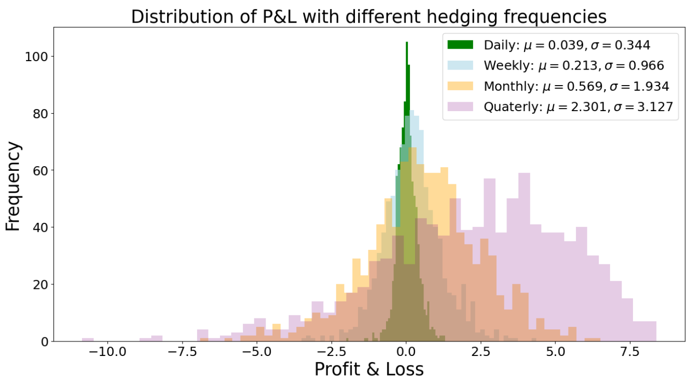

(a) *Distribution of profit-and-loss for different hedging frequencies.*

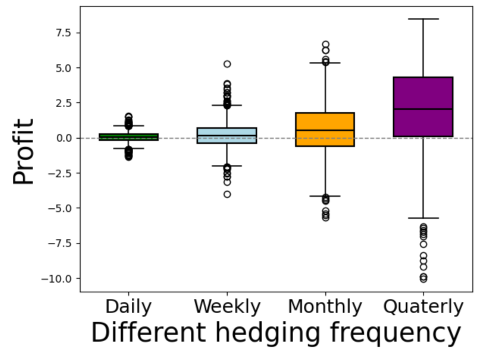

(b) *Box-whisker plot illustrating the median and spread of profit-and-loss for different hedging frequencies.*

Figure 6: Effect of different hedging frequency on the profit-and-loss of the delta-hedging strategy.

50% while fixing the hedging frequency to daily. Finally, we conduct a theoretical analysis to identify the conditions under which mismatched volatility leads to the final profit=and-loss to vanish to zero.

3.3 Results

3.3.1 Effect of different hedging frequency

In Figure 6, we illustrate the effect of different hedging frequencies on the profit-and-loss. In Figure 6(a), we show the distribution of the profit-and-loss for different hedging frequency. We can observe that, regardless of the hedging frequency, most of the hedging frequency have a mean profit-and-loss close to zero. However, as hedging frequency decreases from daily to quarterly, the spread of the profit-and-loss increases, resulting in a non-zero profit-and-loss. This is highlighted by the box-whisker plot in Figure 6(b). Moreover, the full statistics of the P&L statistics for different hedging frequencies are tabulated in Table 4 for reference. These statistics reiterate the fact that daily hedging yields near-zero mean profit-and-loss with low dispersion, whereas less frequent rebalancing produces steadily larger mean profit-and-loss and risk.

Table 4: P&L statistics for different hedging frequencies (n=1000 each).

Frequency	**Mean ± Std**	**95% CI**
Daily	0.0391 ± 0.3440	[0.0177, 0.0604]
Weekly	0.2132 ± 0.9663	[0.1532, 0.2731]
Monthly	0.5689 ± 1.9351	[0.4488, 0.6890]
Quarterly	2.3006 ± 3.1282	[2.1065, 2.4947]

3.3.2 Effect of mismatched volatility

In Figure 7, we illustrate the effect of mismatched volatility of the underlying and delta valuation on the profit-and-loss. In Figure 7(a), we show the distribution of the profit-and-loss for different volatility of delta valuation. We can observe that the delta hedging results in a loss when the delta valuation overestimates the volatility of the the stock while resulting in a profit when the delta valuation underestimates the volatility of

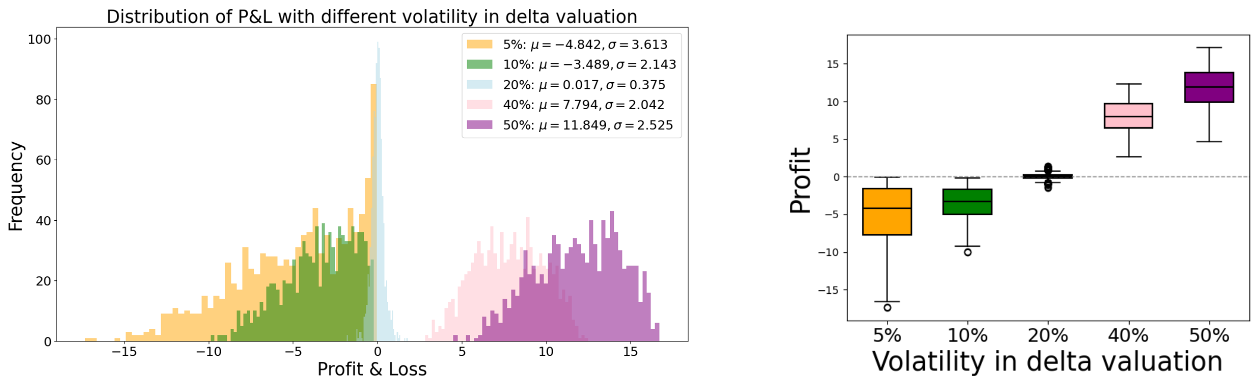

(a) *Distribution of profit-and-loss for different delta valuation volatilities.*

(b) *Box-whisker plot illustrating the median and spread of profit-and-loss for different delta valuation volatilities.*

Figure 7: Effect of mismatched volatility on the profit-and-loss of the delta-hedging strategy.

the the stock. This is further highlighted by the box-whisker plot in Figure 7(b). Moreover, the statistics of the P&L statistics for delta valuation volatilities are tabulated in Table 5. These results again confirm that the mean profit-and-loss is negative when the assumed volatility underestimates the actual realized volatility (e.g. -4.84 at 5%) and positive when it overestimates (e.g. 11.85 at 50%), exactly as dictated by the $(\sigma_{\text{imp}}^2 - \sigma_t^2)$ term in upcoming equation (22).

Table 5: P&L statistics for different delta valuation volatilities (n=1000 each).

Volatility	**Mean ± Std**	**95% CI**
5%	-4.8419 ± 3.6145	$[-5.0662,\ -4.6176]$
10%	-3.4890 ± 2.1444	$[-3.6221,\ -3.3560]$
20%	0.0168 ± 0.3748	$[-0.0065,\ 0.0400]$
40%	7.7938 ± 2.0426	$[7.6670,\ 7.9205]$
50%	11.8488 ± 2.5258	$[11.6921,\ 12.0056]$

3.3.3 Pricing and Hedging with Implied Volatility

Given a vanilla option with value function,

$$
\begin{aligned}
&C(t, S; \sigma_{imp}) = C_t \\
&\quad \text{where,} \quad S \text{ is underlying with spot price } S_t, \text{ and} \\
&\qquad\qquad\quad \sigma_{imp} \text{ is implied volatility}
\end{aligned}
$$

The option is priced under risk-neutral measure $\mathbb{Q}$ by solving the Black-Scholes-Merton PDE with implied volatility σ_{imp}.

$$
rC_t - rS_t \frac{\partial C_t}{\partial S_t} - \frac{\partial C_t}{\partial t} - \frac{1}{2}\sigma_{imp}^2 S_t^2 \frac{\partial^2 C_t}{\partial S_t^2} = 0 \tag{6}
$$

The option delta is given by

$$\Delta_t = \frac{\partial C_t}{\partial S_t}$$

The dynamics of the underlying price S_t under real-world measure $\mathbb{P}$ is given by

$$\frac{dS_t}{S_t} = rdt + \sigma_t dW_t^{\mathbb{P}}$$

where, σ_t is instantaneous realized volatility

Here, we aim to prove that in order for the final P&L to vanish on average, the implied volatility σ_{imp} used for pricing and risk management must, on average, match the future realized volatility σ_t when weighted by the option's dollar gamma over its life.

Proof:

Applying Itô's formula to option value:

$$\begin{aligned} dC_t &= (\frac{\partial C_t}{\partial t} + \frac{1}{2}\sigma_t^2 S_t^2 \frac{\partial C_t^2}{\partial S_t^2})dt + rS_t \frac{\partial C_t}{\partial S_t} dt + \sigma_t S_t \frac{\partial C_t}{\partial S_t} dW_t^{\mathbb{P}} & (7) \\ &= (\frac{\partial C_t}{\partial t} + \frac{1}{2}\sigma_t^2 S_t^2 \frac{\partial C_t^2}{\partial S_t^2})dt + \frac{\partial C_t}{\partial S_t} dS_t & (8) \end{aligned}$$

From the PDE (6),

$$\frac{\partial C_t}{\partial t} = rC_t - rS_t \frac{\partial C_t}{\partial S_t} - \frac{1}{2}\sigma_{imp}^2 S_t^2 \frac{\partial^2 C_t}{\partial S_t^2} \tag{9}$$

Substituting (9) in (8),

$$\begin{aligned} dC_t &= \big(rC_t - rS_t \frac{\partial C_t}{\partial S_t} - \frac{1}{2}\sigma_{imp}^2 S_t^2 \frac{\partial^2 C_t}{\partial S_t^2} + \frac{1}{2}\sigma_t^2 S_t^2 \frac{\partial C_t^2}{\partial S_t^2}\big)dt + \frac{\partial C_t}{\partial S_t} dS_t & (10) \\ &= \big(rC_t - rS_t \frac{\partial C_t}{\partial S_t} - \frac{1}{2} S_t^2 \frac{\partial^2 C_t}{\partial S_t^2}[\sigma_{imp}^2 - \sigma_t^2]\big)dt + \frac{\partial C_t}{\partial S_t} dS_t & (11) \end{aligned}$$

The discounted price $\widetilde{C_t} = e^{-rt} C_t$. By product rule,

$$d\widetilde{C_t} = e^{-rt} dC_t - rC_t e^{-rt} dt \tag{12}$$

Similarly, the discounted asset price $\widetilde{S_t} = e^{-rt} S_t$. By product rule,

$$d\widetilde{S_t} = e^{-rt} dS_t - rS_t e^{-rt} dt \tag{13}$$

Substituting (11) in (12),

$$\begin{aligned} d\widetilde{C_t} &= e^{-rt}\big[\big(rC_t - rS_t \frac{\partial C_t}{\partial S_t} - \frac{1}{2} S_t^2 \frac{\partial^2 C_t}{\partial S_t^2}[\sigma_{imp}^2 - \sigma_t^2]\big)dt + \frac{\partial C_t}{\partial S_t} dS_t\big] - rC_t e^{-rt} dt & (14) \\ &= e^{-rt}\big(- rS_t \frac{\partial C_t}{\partial S_t} - \frac{1}{2} S_t^2 \frac{\partial^2 C_t}{\partial S_t^2}[\sigma_{imp}^2 - \sigma_t^2]\big)dt + e^{-rt} \frac{\partial C_t}{\partial S_t} dS_t & (15) \end{aligned}$$

The instantaneous profit and loss is given by (assuming no dividends $q = 0$)

$$P\&L = -dC_t + rC_t dt + \Delta_t(dS_t - rS_t d_t)$$

Discounting the $P\&L$ and substituting (12) and (13)

$$\widetilde{P\&L} = e^{-rt}(-dC_t + rC_t dt + \Delta_t(dS_t - rS_t d_t)) \tag{16}$$
$$= -d\widetilde{C}_t + \Delta_t d\widetilde{S}_t \tag{17}$$

Substituting $\Delta_t = \frac{\partial C_t}{\partial S_t}$, (13) and(15) in (17),

$$\widetilde{P\&L} = -d\widetilde{C}_t + \Delta_t d\widetilde{S}_t \tag{18}$$
$$= -e^{-rt}\big(-rS_t\frac{\partial C_t}{\partial S_t} - \frac{1}{2}S_t^2\frac{\partial^2 C_t}{\partial S_t^2}[\sigma_{imp}^2 - \sigma_t^2]\big)dt - e^{-rt}\frac{\partial C_t}{\partial S_t}dS_t + \frac{\partial C_t}{\partial S_t}(e^{-rt}dS_t - rS_t e^{-rt}dt) \tag{19}$$
$$= e^{-rt}\frac{1}{2}S_t^2\frac{\partial^2 C_t}{\partial S_t^2}[\sigma_{imp}^2 - \sigma_t^2]dt \tag{20}$$

Therefore, the total $\widetilde{\mathbf{P\&L}}$ is,

$$\widetilde{\mathbf{P\&L}} = \int_0^T e^{-rt}\frac{1}{2}S_t^2\frac{\partial^2 C_t}{\partial S_t^2}[\sigma_{imp}^2 - \sigma_t^2]dt \tag{21}$$

As given by the risk management condition, the average total profit and loss $\widetilde{\mathbf{P\&L}}$ is zero

$$\mathbb{E}[\widetilde{\mathbf{P\&L}}] = \mathbb{E}\big[\int_0^T e^{-rt}\frac{1}{2}S_t^2\frac{\partial^2 C_t}{\partial S_t^2}[\sigma_{imp}^2 - \sigma_t^2]dt\big] = 0 \tag{22}$$

Conclusion

In the first part of this assignment, we carried out a detailed volatility analysis for Microsoft (MSFT). We computed 30-day rolling classical (close-to-close) and Parkinson range-based volatilities, showed both to be highly correlated with option-implied volatility, and demonstrated that the Parkinson estimator is somewhat smoother. We then constructed a model-free VIX estimate at our analysis date, refined it using mid-quotes and strike filters, and compared it to the CBOE-quoted VIX. Finally, regressions of S&P500 returns on the VIX level, realized variance, and changes in the VIX revealed that volatility surprises (changes in VIX) explain the vast majority of daily return variation, whereas static volatility measures add little predictive power.

In the second part, we solved the Black–Scholes partial differential equation for a power payoff $C(S,T) = S^2$. By using the ansatz $C(S,t) = S^2 f(t)$ we reduced the problem to an ordinary differential equation, obtained an explicit closed-form solution, and then derived the corresponding delta and bond holdings for an exact, self-financing replicating portfolio.

In the third part, we simulated discrete-time delta-hedging under both matched and mismatched volatility assumptions. When the hedging volatility matches the true volatility, the expected profit-and-loss is zero but dispersion grows as we hedge less frequently. When the assumed volatility deviates, the strategy incurs systematic losses or gains proportional to the degree of mismatch. We closed with a proof that the expected

P&L of a delta-hedged position vanishes if and only if the assumed (implied) volatility matches the actual future realized volatility when weighted by the option's gamma over its life.

Together, these three tasks highlight (i) the practical behavior of different volatility estimators and their relationship to market expectations, (ii) the power of analytical solutions for precise option pricing and hedging, and (iii) the critical importance of volatility alignment and hedging frequency in managing risk and controlling profit-and-loss outcomes.

References

Black, F., & Scholes, M. S. (1973). The pricing of options and corporate liabilities. *Journal of Political Economy*, *81*(3), 637–654.

Breusch, T. S., & Pagan, A. R. (1979). A simple test for heteroscedasticity and random coefficient variation. *Econometrica*, *47*(5), 1287–1294.

Chicago Board Options Exchange. (2003). CBOE Volatility Index (VIX) white paper [Computer software manual]. (`https://www.cboe.com/micro/vix/vixwhite.pdf`)

Dickey, D. A., & Fuller, W. A. (1979). Distribution of the estimators for autoregressive time series with a unit root. *Journal of the American Statistical Association*, *74*(366), 427–431.

Hull, J. C. (2015). *Options, futures, and other derivatives* (9th ed.). Pearson.

Parkinson, M. (1980). The extreme value method for estimating the variance of the rate of return. *Journal of Business*, *53*(1), 61–65.

Whaley, R. E. (2000). The investor fear gauge. *The Journal of Portfolio Management*, *26*(3), 12–17.